Decision Analytics Journal 8 (2023) 100312

Contents lists available at ScienceDirect

Decision Analytics Journal

journal homepage: www.elsevier.com/locate/dajour

A service network design for scheduled advanced air mobility using human-driven and autonomous air metro

Runqing Zhao [a,b,*], Tay T.R. Koo [a], Wei Liu [c], Gabriel Lodewijks [a,d], Fangni Zhang [a,e]

[a] School of Aviation, University of New South Wales, Sydney, Australia
[b] Intelligent Transportation Thrust, The Hong Kong University of Science and Technology (Guangzhou), Guangzhou, China
[c] Department of Aeronautical and Aviation Engineering, The Hong Kong Polytechnic University, Hong Kong, China
[d] School of Engineering, The University of Newcastle, Newcastle, Australia
[e] Department of Industrial and Manufacturing Systems Engineering, University of Hong Kong, Hong Kong, China

ARTICLE INFO

Keywords:
Advanced air mobility
Air metro
Autonomous vertical take-off and landing
Rolling horizon optimisation
Time-space network

ABSTRACT

Emerging modes of advanced air mobility are potential alternatives to current ground transport. This study proposes a service network design approach for the air metro, a pre-scheduled service with fixed routes that accommodate passengers for intra- or inter-city trips. The scenarios of human-driven and autonomous air metro are then compared, where the former has a labour cost for pilots and the latter has a higher capital costs such as vehicle and automation costs. Then, a rolling horizon optimisation approach is proposed, where the temporal length of a single rolling horizon is an early confirmation period plus a safety margin. The rolling horizon introduces decision and marginal arcs with different fleet, passenger, and pilot network capabilities. The optimised outputs on critical arcs are determined and fixed, while the marginal arcs can be continuously adjusted in the subsequent rolling horizons. Numerical studies are undertaken across all variables in the context of the Greater Metropolitan Area of Sydney, Australia. Results suggest that the human-driven air metro would be economically preferable until the utilisation cost of an autonomous aircraft can reduce by 60%. Furthermore, confirming the actual passenger demand at least 45 min in advance is recommended, and a single rolling horizon should be longer than 150 min.

1. Introduction

The emerging concept of advanced air mobility (AAM) has recently been proposed as potential inter- or intra-city passenger transport services with vertical take-off and landing (VTOL) aircraft.[1] AAM complements public transport, functions cooperatively with rail, metro, and bus stations, and alleviates urban traffic congestion. It offers disruptive innovation not only to the air transport, but also to the urban mobility market [2]. The market value of advanced modes of air transport providers in the U.S. alone is forecast by some analysts to be in excess of $283b within 20 years; at first the services are likely to be costly, but since the ride-sharing model amortises vehicle costs over a large number of paid-trips, the high cost is unlikely to prove prohibitive to launching the service [3]. It is estimated that approx. 98% of the demand of its market are trips greater than 30 min in travel time served by ground transport [4]. Reiche et al. [5] estimated the potential demand for the emerging modes in the U.S. to be 0.1% of all trips. Due to AAM's enormous market potential, multiple commercial companies are making efforts to assess advanced air services, such as Uber [6], Porsche [7], Airbus [8], etc.

As part of NASA's analysis of the potential for AAM, several options were proposed, including last-mile delivery, air metro, air taxi, etc. [5,9,10]. Air metro is defined as a public transport alternative for thin-haul commuters [11], with fixed schedules prior to flight departure. Hasan [9] suggested that the air metro would enjoy a profitable first year in 2028 where there would be 130 m passenger trips annually (assuming a market exists) and the break-even cost is expected to be approx. $6.2b. Moreover, air metro has a lower density for vertiports than the air taxis, which is about 100–300 vertiports per metropolitan statistical area in high traffic areas.

Prior to committing investment, service network design problem (SNDP) are often studied to analyse the main types of costs, and to determine the range of optimal dispatch patterns to establish a design for a potential service network [e.g., 12]. This provides useful information for decision making and analytically constructed scenario planning tools. In order to understand and simulate the viability of a

* Corresponding author at: Intelligent Transportation Thrust, The Hong Kong University of Science and Technology (Guangzhou), Guangzhou, China.
E-mail address: rzhao820@connect.hkust-gz.edu.cn (R. Zhao).

[1] Air metro and air taxis are developed beyond the urban landscape, serving suburbs and rural area and the term "urban" falls short of encompassing the concepts of the advanced air mobility [1]. We use "advanced air mobility" to represent similar concepts such as "urban air mobility".

https://doi.org/10.1016/j.dajour.2023.100312
Received 14 November 2022; Received in revised form 19 May 2023; Accepted 30 August 2023
Available online 4 September 2023

novel service network, it is necessary to consider the tactical decision. This involves the objective of reducing, or balancing, service provider's costs and passengers' journey times.

This paper aims to design a service network for the air metro using time-space networks (TSNs) to compare the economic feasibility of autonomous and human driven AAM service networks by determining the optimal fleet size and dispatch patterns. We achieve the objective through the following steps. We firstly design service networks for an autonomous scenario - a technologically feasible operation with autonomous aviation and a feature that AAM developers are seriously considering. In light of the fact that pilot availability is regulated by work hours (start and end duty times), focusing on a human-driven air metro scenario introduces an additional layer of pilot scheduling and provides an opportunity to investigate the trade-off between human-driven and autonomous air metros. The scheduled air metro is operated and managed differently from on-demand air taxis. On-demand air taxi service is provided based on the fully known demand, while the plan of pre-scheduled air metro is made before the demand date acquisition; that is, the demand is unknown or only partially known. Then, the human-driven air metro is extended to incorporate demand stochasticity, by developing a dynamic optimisation in rolling horizon. The rolling horizon is particularly efficient when the passenger demand for the "near future" is available while the demand in the "far future" is predicted according to the historical distribution in each rolling horizon. Lastly, using the developed models, the paper conducts a numerical study of an inter-city passenger network based on Greater Metropolitan Area of Sydney (GMAS) to illustrate the modelling approach and assess the cost feasibility of conventionally human-driven VTOL fleets (pilot onboard) versus autonomous fleets.

This paper adds to the literature in several ways. First, to the best of authors' knowledge, this is the first study that specifically focuses on air metro, instead of its counterpart in AAM systems, namely air taxi. Second, this study jointly optimises the AAM fleet scheduling and pilot scheduling, enabling an analysis of human driven v.s. autonomous scenarios. Third, considering the unique operational features of air metro (e.g., the operation can be centrally controlled), a proper rolling horizon approach is proposed.

The rest of this paper is organised as follows. Section 2 reviews the existing studies related to the modelling approach of AAM service network. Section 3 explicates the TSNs and formulates the optimisation model for the air metro service network in autonomous and human driven scenarios. Following this, the rolling horizon modelling approach is introduced. Section 4 includes a case study of the GMAS. Section 5 concludes.

2. Literature review

The close collaboration between demand modelling, network design, and physical system development is important for reliable, efficient, and safe integration of AAM [13]. AAM provides potential travel time savings. As is well known in travel demand studies, there is a trade-off between travel time savings and air fare willingness. Previous studies mainly focus on the impact of ground autonomous vehicles on the value of time (VOT) [e.g., 14], acceptability for autonomy [e.g., 15], preferences on mode choice [e.g., 16]. These results are particularly relevant to AAM demand and pricing [17]. Through a survey of passengers' adoption of flying cars, Eker et al. [18] revealed that various socio-demographic characteristics, individual-specific behavioural, driving attributes, and attitudinal perspectives affect the willingness to pay for and use flying cars. Moreover, in the autonomous AAM context, the level of autonomy markedly affects the market attractiveness [19]. Assuming fully autonomous air vehicles, Al Haddad et al. [20] identified and quantified the factors that affect the adoption and use of AAM. These included perceived safety, perceived benefits, as well as general willingness to accept new technology.

At a strategic and supply level, an AAM network is established by considering the design and placement of vertiports. Schweiger and Preis [21] conducted a systematic review finding that there are 49 publications covering the topics related to AAM ground infrastructure and airspace operation including design, location, capacity, etc. Shao et al. [22] proposed an adaptive control system for the terminal area of the multi-vertiport system, including the design of the operating environment and the integrated scheduling model. Strategic-level studies have influenced the development of AAM service network studies. The vertiport location placement problem has received the most attention at strategic level [23–28]. For example, Sinha and Rajendran [26] proposed a unique two-phase procedure that integrates the multi-criteria warm start technique with an iterative k-means clustering algorithm, to optimise the vertiport location. In all, the operations of vertiports require an analysis of the land use, regional demand, availability of space, local economic factors, commute time, and service coverage range [29].

AAM service network are also studied at a tactical level. Roy et al. [30] modelled the on-demand air taxi service through a multi-commodity network flow approach. The results provided the optimal fleet size and identified the factors that have significant impact on operating cost and profitability. Rajendran [31] developed a hybrid simulation goal programming algorithm that comprehensively incorporates the problems at different levels, including the fleet size, passenger time cost, and real-time dispatch patterns. [32] proposed models and algorithms to schedule the air taxi fleet to meet the expected arrival time at vertiports, while attempting to optimise routing and battery recharging tasks. The emerging modes of AAM are also studied in the context of air ambulance [e.g., 33] and airport shuttle [e.g., 34]. However, modelling approaches have not attracted sufficient development at all aspects of the tactical decisions. Willey and Salmon [25] modelled the vertical placement problem as a single-allocation p-hub median location problem that incorporates aspects important to the operation of transport networks to make the vertiports suitable for use by air metro system. Tactical air metro service network studies based on the strategic vertiport location decisions are still required.

This paper attempts to develop a service network design at a tactical level (assuming the strategic level decisions such as vertiport placements have already been made) for a scheduled air metro service in the context of Sydney, Australia. Specifically, the following three modelling gaps are to be addressed in this paper. First, when studying the dispatch pattern of AAM service, pilot scheduling has not been considered as an endogenous factor in the models of existing studies. Thus, pilot scheduling requires a dimension in the joint optimisation with fleet scheduling. Second, although autonomous aviation is expected to be achieved in not-too-distant future, and some studies have already implicitly assumed fully autonomous aircraft in AAM, there has not been a study for the comparison of operating cost between human driven and autonomous AAM service. Third, the concept of rolling horizon optimisation has not been widely utilised in the topic of AAM. In most existing rolling horizon optimisation studies relating to transport systems, the focus is on bus operation, where once dispatched from the origin, a vehicle's schedule remains unchanged [e.g., 35]. The only application of rolling horizon optimisation on AAM is a VTOL arrival scheduling study [36]. Focusing on the tactical level decisions of AAM, this study will address the above gaps in the service network design of air metro.

3. Problem description & formulation

This study optimises the dispatch patterns at a tactical level, where all the strategic decisions are given; that is, vertiports are assumed to be already established and available with fixed positions before the fleet size is determined.

3.1. Static formulation for unknown demand scenario

In this section, we firstly model the proposed service as an ILP, under the assumptions that the passenger demand is deterministic.

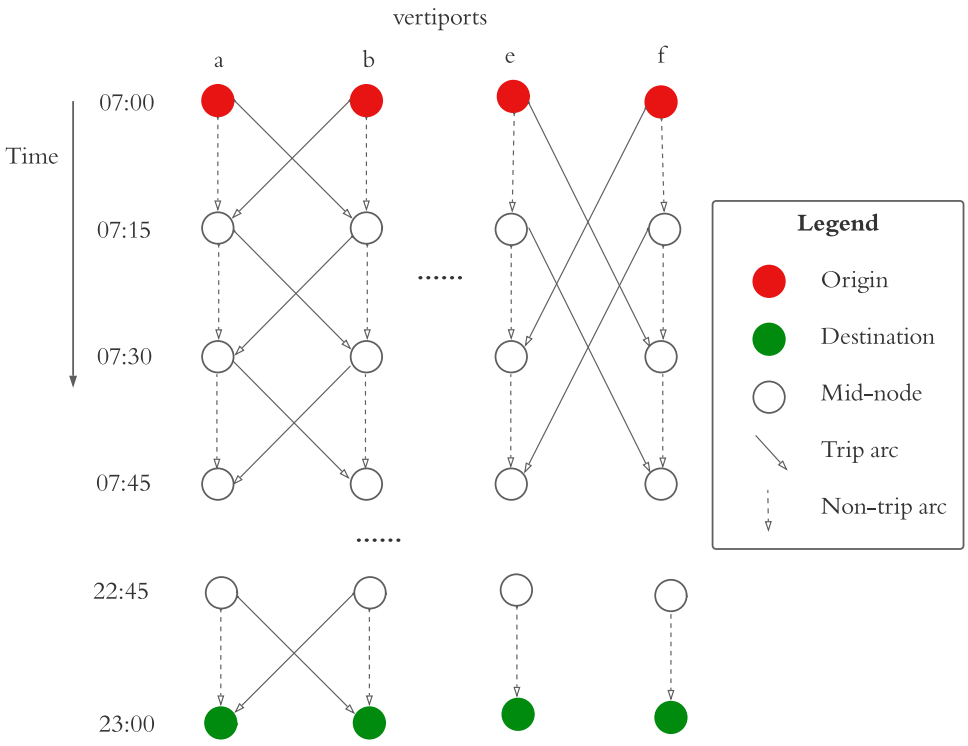

Fig. 1. An example for the FLT-TSN.

3.1.1. Problem description

There are different types of TSNs available for multi-commodity models. For example, the TSNs developed by Lo et al. [37] considered the aggregate passenger groups and did not require a searching process of potential feasible itineraries, while the TSNs for itinerary-based models [e.g., 38,39] requires searching feasible itineraries and is more suitable for dial-a-ride problem or on-demand air taxis. Thus, we refer to the TSNs developed by Lo et al. [37] to establish the modelling framework.

Let $(\mathcal{N}, \mathcal{A})$ denote the general network graph that simulates the entire planning horizon, where $\mathcal{N}$ is the set of nodes and $\mathcal{A}$ is the set of arcs. To model the movement of passengers, pilots, and fleets, we use directed graphs that specifies the time and space dimensions, referred as a fleet flow time-space network (FLT-TSN), a collection of passenger flow time-space networks (PAX-TSNs) and a collection of pilot flow time-space networks (PLT-TSNs), respectively. Arcs are used to specify the VTOL fleet flow, passenger flow and pilot flow movements in the corresponding TSNs. Passenger groups are coined according to their OD pairs, their arrival time at origin vertiport, and their tolerable latest arrival time at the destination. Accordingly, we define each passenger group as a time-dependent origin–destination pair (TDODP). The arrival time constraints at the destination vertiports are incorporated into the tailored PAX-TSNs of the TDODPs. During the period of service, we assume that the VTOLs do not maintain fixed depots.

Fleet flow

A planning period only requires one FLT-TSN. Commonly, a time step is relatively small compared with other time parameters (e.g., travel time between two nodes, waiting time of passenger at a vertiport), it is considered to be the unit of time parameters. Thus, all time-related parameters become the integral multiples of the time step. A trip arc $(i, j) \in \mathcal{R}^f$ represents a trip of an air metro, associated with an non-negative operating cost. The operating cost on non-trip arcs can be negligible. Fig. 1 shows a FLT-TSN installed with n vertiports as an example. In this example, a time-step of 15 min is adopted, and thus the trip times between the nodes are estimated to be multiples of 15 min (e.g., 15, 30, 45 min).

Pilot flow

For pilot operations, a duty is a duration within a working day of a pilot and consists of a sequence of consecutive flights, connections (transition time between flight legs) and deadheads. We assume that the pilots also do not have fixed depots during the duty period. Pilot flows are segregated into different networks, which can also vary in size. For each arc, a non-negative integer variable represents the pilot movement. The PLT-TSNs have the similar shape to FLT-TSNs in Fig. 1, where most nodes and arcs from the general graph $(\mathcal{N}, \mathcal{A})$ are applicable to each PLT-TSN, as long as the duty time window are satisfied. Hence, fleet flow, passenger flow and pilot flow constitute the three dimensions of TSNs in this study: a FLT-TSN, a set of PAX-TSNs, and a set of PLT-TSNs.

Passenger flow

A PAX-TSN is associated with a specific passenger group, specifically tailored according to the TDODP. Thus, each PAX-TSN can vary in size, and only a portion of the nodes and arcs from the general network graph are applicable to each PAX-TSN, depending on the arrival time window and the feasibility of the trip. Once some passengers enter the network, they must be transported by the service, otherwise, the service is penalised.

Fig. 2 shows examples of PAX-TSNs. The exogenous demand for a TDODP occurs once. As specified by the corresponding nodes, an oblique arc indicates a trip leg between two vertiports; while on vertical arc, the flows represent the number of passengers waiting at the vertiport. For the example in Fig. 2(a), passengers have a maximum acceptable journey time of 45 min. The destination is the vertiport b. Thus, all nodes belonging to column b are the destination.

Table 1 specifies the nomenclature and abbreviations used in the model.

3.1.2. Autonomous air metro formulation

In this section, we examine modelling approach for the autonomous air metro scenario, where the service is provided by autonomous VTOLs. Hence, the labour cost of pilots is not taken into consideration

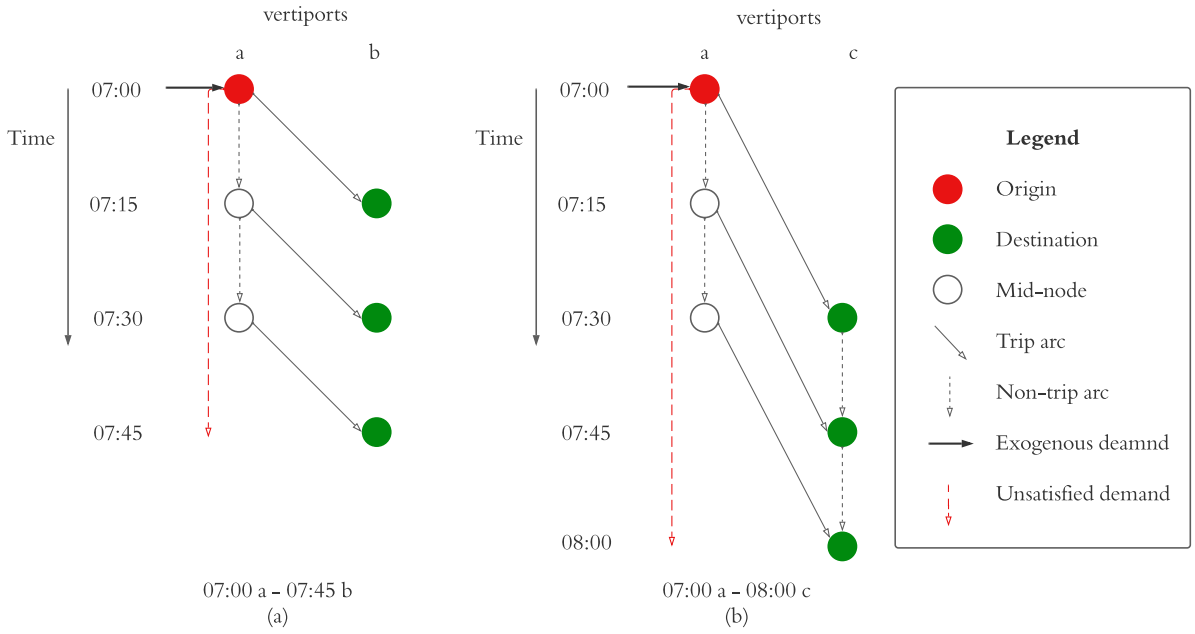

Fig. 2. Examples for PAX-TSNs.

Table 1
Nomenclature.

Symbol	Definition
Indices & sets	
$\mathcal{B}$	Set of the TDODPs
b	The bth PAX-TSN, corresponding to a TDODP, a member of $\mathcal{B}$
$\mathcal{E}$	Set of pilot duty period within a working day
e	The eth PLT-TSN, a member of $\mathcal{E}$
$\mathcal{M}^b, \mathcal{M}^e, \mathcal{M}^f$	Set of nodes at the middle of the planning period in the bth PAX-TSN, the eth PLT-TSN, and the FLT-TSN, respectively
$\mathcal{D}^f$	Set of nodes at the end of the planning period in the FLT-TSN
$\mathcal{A}^b, \mathcal{A}^e, \mathcal{A}^f$	Sets of arcs in the bth PAX-TSN, the eth PLT-TSN, and the FLT-TSN, respectively
$\mathcal{O}^b, \mathcal{O}^e, \mathcal{O}^f$	Set of arcs beginning at the start nodes in the bth PAX-TSN, the eth PLT-TSN, and the FLT-TSN, respectively
$\mathcal{P}(i)$	Set of arcs ending at node i
$\mathcal{Q}(i)$	Set of arcs starting at node i
$\mathcal{R}^e, \mathcal{R}^f$	Set of trip arcs in the eth PLT-TSN, the FLT-TSN, respectively
Definitional parameters	
B^b	Exogenous passenger demand for the bth PAX-TSN
C	Capacity of a VTOL
V	Capacity of vertiports, i.e, the maximum number of VTOLs landing at a vertiport at the same time-step
E	Pilot salary for the planning horizon
F	Fleet size
J	Utilisation cost of a VTOL for serving the planning time period
R_{ij}	Operating cost for a VTOL's trip on arc (i, j)
T_{ij}	Monetary travel time between nodes i and j
P	Penalty for a unsatisfied passenger
Decision variables	
w_{ij}^b	Integer variable that indicates the number of passengers of the bth TDODP on arc (i, j)
x_{ij}^e	Integer variable that indicates the number of pilots on arc (i, j) of the eth PLT-TSN
y_{ij}	Integer variable that indicates the number of VTOLs on arc (i, j)
z^b	Number of unsatisfied passengers for the bth PAX-TSN

and the pilot scheduling is exempted. The deterministic passenger demand is obtained according to historical average. Then, an optimisation model for the autonomous air metro, i.e., **(P0)**, is

$$\min_{\mathbf{w},\mathbf{y},\mathbf{z}} \sum_{b\in\mathcal{B}} \Big(\sum_{ij\in\mathcal{A}^b} w_{ij}^b T_{ij} + z^b P \Big) + \sum_{ij\in\mathcal{R}^f} y_{ij} R_{ij} + \sum_{ij\in\mathcal{O}^f} y_{ij} J \tag{1}$$

subject to

$$\sum_{ij\in\mathcal{O}^b} w_{ij}^b = B^b - z^b \quad \forall b \in \mathcal{B} \tag{2}$$

$$\sum_{ij\in\mathcal{Q}(i)} w_{ij}^b - \sum_{ki\in\mathcal{P}(i)} w_{ki}^b = 0 \quad \forall b \in \mathcal{B} \quad \forall i \in \mathcal{M}^b \tag{3}$$

$$\sum_{b\in\mathcal{B}} w_{ij}^b \leqslant y_{ij} C \quad \forall ij \in \mathcal{R}^f \tag{4}$$

$$\sum_{ij\in\mathcal{Q}(i)} y_{ij} - \sum_{ki\in\mathcal{P}(i)} y_{ki} = 0 \quad \forall i \in \mathcal{M}^f \tag{5}$$

$$\sum_{ki\in\mathcal{P}(i)} y_{ki} \leqslant V \quad \forall i \in \mathcal{M}^f \cup \mathcal{D}^f \tag{6}$$

$$\sum_{ij\in\mathcal{O}^f} y_{ij} \leqslant F \tag{7}$$

$$w_{ij}^b \in \mathbb{N} \quad \forall b \in \mathcal{B} \quad \forall ij \in \mathcal{A}^b \tag{8}$$

$$y_{ij} \in \mathbb{N} \quad \forall ij \in \mathcal{A}^f \tag{9}$$

Table 2
Nomenclature.

Symbol	Definition
$[1,\dots,H]$	Rolling horizons
$\mathcal{N}_h, \mathcal{A}_h$	Sets of active nodes and active arcs in the rolling horizon h, respectively
$\mathcal{B}_h, \mathcal{E}_h$	Active PAX-TSNs and PLT-TSNs considered in the rolling horizon h, respectively
$\mathcal{V}_h$	PLT-TSNs share the start time with the rolling horizon h
$\mathcal{M}^b_h, \mathcal{M}^e_h, \mathcal{M}^f_h$	$\mathcal{M}^b \cap \mathcal{N}_h, \mathcal{M}^e \cap \mathcal{N}_h, \mathcal{M}^f \cap \mathcal{N}_h$, respectively
$\mathcal{A}^b_h, \mathcal{A}^e_h, \mathcal{A}^f_h$	$\mathcal{A}^b \cap \mathcal{A}_h, \mathcal{A}^e \cap \mathcal{A}_h, \mathcal{A}^f \cap \mathcal{A}_h$, respectively
$\mathcal{O}^b_h, \mathcal{R}^e_h, \mathcal{R}^f_h$	$\mathcal{O}^b \cap \mathcal{A}^b_h, \mathcal{R}^e \cap \mathcal{A}^e_h, \mathcal{R}^f \cap \mathcal{A}^f_h$, respectively
$\mathcal{P}_h(i), \mathcal{Q}_h(i)$	$\mathcal{P}(i) \cap \mathcal{A}_h, \mathcal{Q}(i) \cap \mathcal{A}_h$, respectively
$\tilde{\mathcal{P}}_h(i)$	Set of decided arcs ending at node i, on which the decisions are made during $[1,\dots h-1]$
$\tilde{w}^b_{ij,h}$	Number of passengers of the bth TDODP on decided arc (i,j) determined during $[1,\dots h-1]$
$\tilde{x}^e_{ij,h}$	Number of pilots on decided arc (i,j) of the eth PLT-TSN determined during $[1,\dots h-1]$
$\tilde{y}_{ij,h}$	Number of VTOLs on decided arc (i,j) determined during $[1,\dots h-1]$
$u_{ij,h}$	Integer variable that indicates number of newly added VTOLs into the network on active arc $(i,j) \in \mathcal{R}^f_h$
$v^e_{ij,h}$	Integer variable that indicates number of newly added pilots into the network on active arc $(i,j) \in \mathcal{R}^e_h$, $e \in \mathcal{V}_h$
$w^b_{ij,h}$	Integer variable that indicates the number of passengers on arc $(i,j) \in \mathcal{A}^b_h$, $b \in \mathcal{B}_h$
$x^e_{ij,h}$	Integer variable that indicates the number of pilots on arc $(i,j) \in \mathcal{A}^e_h$, $e \in \mathcal{V}_h$ which have started their duty during $[1,\dots h-1]$
$y_{ij,h}$	Integer variable that indicates the number of VTOLs on active arc $(i,j) \in \mathcal{A}^f_h$ which have started their service during $[1,\dots h-1]$

$$z^b \in \mathbb{N} \quad \forall b \in \mathcal{B} \tag{10}$$

where $\mathbf{w} = \{w^d_{ij}\}$, $\mathbf{y} = \{y_{ij}\}$, $\mathbf{z} = \{z^b\}$.

The objective function (1) minimises the total system cost, which includes both the monetary passenger journey time and operating costs. The objective function has three terms: (i) passengers' monetary time cost, including waiting and in-vehicle travel time; (ii) air metro operating cost (e.g., energy cost, battery reserve cost); (iii) VTOLs' utilisation cost (e.g., depreciation of a capital asset). Constraint (2) inputs the exogenous passenger demand to each PAX-TSN. Constraint (3) ensures the passenger flow conservation at each node. Constraint (4) restricts the number of passengers on each service arc to no more than its maximum capacity $y_{ij}C$. Constraint (5) ensures the VTOL fleet flow conservation at each node. Constraint (6) sets the number of VTOLs put into use is no more than the fleet size (VTOLs not been put into use could be stocked at warehouse). Constraint (7) sets the maximum allowable in-flows of air metro at each vertiport (e.g., due to vertiport capacity constraint). Constraint (8)–(9) set the number of passengers and VTOLs to be non-negative integers. The model optimises the number of passengers in PAX-TSNs $\mathbf{w}$ and the number of VTOLs in FLT-TSNs $\mathbf{y}$ in the air metro service network, to minimise the total system cost in Eq. (1). The model constitutes an ILP that is solvable by commercial solvers (e.g., Gurobi).

3.1.3. Human driven air metro formulation

In this section, an additional dimension for pilot scheduling is added into the optimisation model. One needs to hire a fleet of VTOLs and employ pilots. Compared with the autonomous air metro model, the objective function for the human driven air metro, i.e., (**P1**), can be revised as follows:

$$\min_{\mathbf{w},\mathbf{x},\mathbf{y},\mathbf{z}} \sum_{b\in\mathcal{B}} \Big(\sum_{ij\in\mathcal{A}^b} w^b_{ij} T_{ij} + z^b P \Big) + \sum_{ij\in\mathcal{R}^f} y_{ij} R_{ij} + \sum_{ij\in\mathcal{O}^f} y_{ij} J + \sum_{e\in\mathcal{E}} \sum_{ij\in\mathcal{O}^e} x^e_{ij} E \tag{11}$$

Constraint (4) can be revised to require that the total number of passengers and pilots on each service arc is no more than the supplied capacity $y_{ij}C$, as shown by following equation:

$$\sum_{b\in\mathcal{B}} w^b_{ij} + \sum_{e\in\mathcal{E}} x^e_{ij} \leqslant y_{ij} C \quad \forall ij \in \mathcal{R}^f \tag{12}$$

Constraints ensuring the feasibility of pilot movement can be added as follows:

$$y_{ij} \leqslant \sum_{e\in\mathcal{E}} x^e_{ij} \quad \forall ij \in \mathcal{R}^f \tag{13}$$

$$\sum_{ij\in\mathcal{Q}(i)} x^e_{ij} - \sum_{ki\in\mathcal{P}(i)} x^e_{ki} = 0 \quad \forall e \in \mathcal{E} \quad \forall i \in \mathcal{M}^e \tag{14}$$

$$x^e_{ij} \in \mathbb{N} \quad \forall e \in \mathcal{E} \quad \forall ij \in \mathcal{A}^e \tag{15}$$

Constraint (13) ensures that each VTOL must have at least one pilot on the service arcs. Constraint (14) ensures the conservation of pilot number at each node in PLT-TSNs. Constraint (15) sets the pilot number to be non-negative integer. Other constraints are to be interpreted in same ways as those (i.e., Eqs. (2)–(3) and (5)–(9)) in (**P0**).

3.2. Rolling horizon formulation for partially known demand scenario

In this section, a dynamic optimisation for human driven air metro in rolling horizon is examined. The fact that the SNDP for the entire day's operations is large and that passenger demand might not be recurrent and fully predictable means a rolling horizon model from a dynamic perspective can be more effective and practical. In the rolling horizon approach, the duration of the day's operations is split into discrete time slice, similar to the time step concept. However, a single rolling horizon (e.g., a 2-h period) can contain several time steps (e.g., a 15-min step). The dispatch patterns in certain time steps are allocated to a rolling horizon. At the start of each rolling horizon, dispatch patterns in time steps belonging to this rolling horizon are determined simultaneously by solving an ILP with a combinatorial passenger demand pattern. In practice, the rolling horizon optimisation is akin to asking passengers to confirm their trips via phone apps a certain hours before departure (e.g., if some customers hope to take air metro that departs at 8 a.m., they need to confirm the trip 2 h in advance, at 6 a.m.), and then the seat would be locked for the passenger. Therefore, the actual demand in the near future is known (e.g., 2-h period); while beyond this time interval, the demand is assumed as the predicted value. We define this time period (e.g., 2 h) as an early confirmation period (ECP). Moreover, we assume that at the beginning of the ECP (e.g., 2 h prior to the departure), there is an accept/reject system to quickly inform passengers whether their requests can be serviced. If the request is rejected, there would be penalty on AAM system total cost. This setting is proper for the management for regional air transport service [38]. A subscript h is added to some notations to indicate the articular rolling horizons. Table 2 further specifies the revised and newly added notations used in the rolling horizon model.

For ease of presentation, we take the FLT-TSNs in rolling horizon as an example to interpret the changes of network graphs. Fig. 3 shows an example with a 30-min period of ECP. At a rolling horizon h starting at 07:15, if the ECP is set to be 30 mins, the actual passenger demand for TDODPs whose departure time is within ECP [07:15, 07:45) is available. A safety margin [07:45, 08:15) is then introduced to achieve a smooth transition between multiple time steps. Thus, the length of rolling horizon is the ECP plus a safety margin, i.e., [07:15, 08:15), which is 60 min in total (in reality, ECP and simulated length could be longer. We use the toy values for interpretation purposes). While a short rolling horizon reduces the computation complexity, a long safety margin can ensure the reliability of solutions.

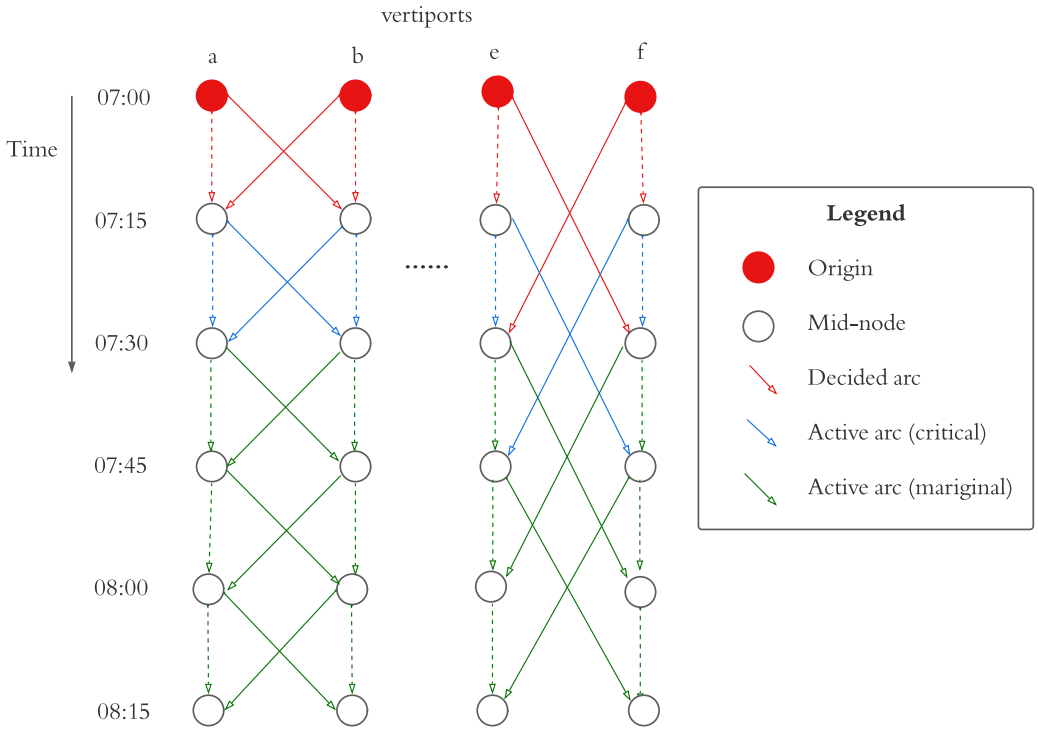

Fig. 3. An example for the FLT-TSN in the rolling horizon.

We further distinguish decided arcs, critical arcs and marginal arcs for a FLT-TSN, where decided arcs is connection between h and $h-1$, $h-2$, etc., on which the decision variables have been decided and cannot be changed. The critical arcs in Fig. 3 are the ones that depart at 07:15, where the flows are determined at h and will not be changed in the subsequent rolling horizons. Although fleet flows for marginal arcs whose departure time are between [07:30, 08:15) are determined, they can be further changed in the next rolling horizons $(h+1, h+2, etc.)$ to suit the actual demand. The set of active arcs for a TSN is the union set of critical and marginal arcs. The decided, critical, marginal and active arcs are distinguished in the same way in PAX-TSNs and PLT-TSNs.

The rolling horizon optimisation framework for air metro consists of multiple models for each rolling horizon. To mathematically formulate the problem for a single rolling horizon h, we make the following assumptions, to make basic settings and identify the active passenger and pilot groups in rolling horizons, i.e., $\mathcal{B}_h, \mathcal{E}_h$: (i) the number of VTOLs offering service in the planning period can increase or decrease at any rolling horizon, however, once it works, the utilisation cost for the planning period occurs; (ii) the number of pilots can varies at any rolling horizon, however, all the pilots that have worked are paid with the salary for the planning horizon; (iii) if expected arrival time window for a PAX-TSN b is within a rolling horizon h, then $b \in \mathcal{B}_h$; (iv) if the flow on any arc in a PLT-TSN e can be determined in h, then the $e \in \mathcal{E}_h$.

Then, an optimisation model for the problem in each rolling horizon h, i.e., problem **(P2)**, is

$$\min_{\mathbf{u}_h,\mathbf{v}_h,\mathbf{w}_h,\mathbf{x}_h,\mathbf{y}_h,\mathbf{z}} \sum_{b\in\mathcal{B}}\Big(\sum_{ij\in\mathcal{A}^b} w^b_{ij}T_{ij} + z^b P\Big) + \sum_{ij\in\mathcal{R}^f_h}(u_{ij,h}+y_{ij,h})R_{ij} + \sum_{ij\in\mathcal{R}^f_h} u_{ij,h}J + \sum_{e\in\mathcal{E}}\sum_{ij\in\mathcal{R}^e_h} v^e_{ij,h}E \tag{16}$$

subject to

$$\sum_{ij\in\mathcal{O}^b_h} w^b_{ij} = B^b_h - z^b \quad \forall b\in\mathcal{B}_h \tag{17}$$

$$\sum_{ij\in\mathcal{Q}_h(i)} w^b_{ij,h} - \sum_{kj\in\mathcal{P}_h(i)} w^b_{ki,h} - \sum_{ki\in\bar{\mathcal{P}}_h(i)} \bar{w}^b_{ki,h} = 0 \quad \forall b\in\mathcal{B} \quad \forall i\in\mathcal{M}^b_h \tag{18}$$

$$\sum_{b\in\mathcal{B}_h} w^b_{ij,h} + \sum_{e\in\mathcal{E}_h} x^e_{ij,h} \leqslant (u_{ij,h}+y_{ij,h})C \quad \forall ij\in\mathcal{R}^f_h \tag{19}$$

$$\sum_{ij\in\mathcal{Q}_h(i)} y_{ij,h} - \sum_{ki\in\mathcal{P}_h(i)}(u_{ki,h}+y_{ki,h}) - \sum_{ki\in\bar{\mathcal{P}}_h(i)} \bar{y}_{ki,h} = 0 \quad \forall i\in\mathcal{M}^f_h \tag{20}$$

$$\sum_{ij\in\mathcal{Q}_h(i)}(u_{ij,h}+y_{ij,h}) \leqslant \sum_{e\in\mathcal{V}_h} v^e_{ij,h} + \sum_{e\in\mathcal{E}_h} x^e_{ij,h} \quad \forall ij\in\mathcal{R}^f_h \tag{21}$$

$$\sum_{ij\in\mathcal{Q}_h(i)} x^e_{ij,h} - \sum_{ki\in\mathcal{P}_h(i)}(v^e_{ki,h}+x^e_{ki,h}) - \sum_{ki\in\bar{\mathcal{P}}_h(i)} \bar{x}^e_{ki,h} = 0 \quad \forall e\in\mathcal{E}_h \quad \forall i\in\mathcal{M}^e_h \tag{22}$$

$$\sum_{ki\in\mathcal{P}_h(i)}(u_{ki,h}+y_{ki,h}) + \sum_{ki\in\bar{\mathcal{P}}_h(i)} \bar{y}_{ki,h} \leqslant V \quad \forall i\in\mathcal{M}^f\cup D^f \tag{23}$$

$$u_{ij,h}, y_{ij,h} \in \mathbb{N} \quad \forall ij\in\mathcal{A}^f_h \tag{24}$$

$$v^e_{ij,h} \in \mathbb{N} \quad \forall e\in\mathcal{V}_h \quad \forall ij\in\mathcal{A}^e_h \tag{25}$$

$$w^b_{ij,h} \in \mathbb{N} \quad \forall b\in\mathcal{B}_h \quad \forall ij\in\mathcal{A}^b_h \tag{26}$$

$$x^e_{ij,h} \in \mathbb{N} \quad \forall e\in\mathcal{E}_h \quad \forall ij\in\mathcal{A}^e_h \tag{27}$$

where $\mathbf{u}_h = \{u_{ij,h}\}$, $\mathbf{v}_h = \{v^e_{ij,h}\}$, $\mathbf{w}_h = \{w^b_{ij,h}\}$, $\mathbf{x}_h = \{x^e_{ij,h}\}$, and $\mathbf{y}_h = \{y_{ij,h}\}$, $\mathbf{z} = \{z^b\}$.

The objective function (16) is to minimise the total system cost under each rolling horizon. Eq. (17) inputs the passenger demand of each PAX-TSN, where B^b_h is a pre-set parameter, equal to B^b if $\mathcal{O}^b_h \neq \emptyset$; or equal to 0 if $\mathcal{O}^b_h = \emptyset$. Eq. (18) requires passenger flow conservation considering the input flow on decided arcs. Eq. (19) requires passenger flow conservation considering the flow on decided arcs. Eq. (20) requires VTOL number conservation considering the value on decided arcs as well as the newly added VTOLs. Eq. (21) ensures the number of pilots on each trip arc considering the newly added VTOLs and pilots. Similar to Eq. (20), Eq. (22) requires pilot number conservation considering the number on decided arcs as well as the newly added pilots into the network. Eq. (23) set the vertiport capacity considering

Table 3
Latitude and longitude of selected vertiports.

Vertiport	Site	Latitude	Longitude
1#	Sydney central	−33.87084	151.20733
2#	Wollongong	−34.42483	150.89311
3#	Newcastle	−32.92827	151.78168
4#	Gosford	−33.42667	151.34167
5#	Woolwich	−33.84029	151.17063
6#	Cronulla	−34.05166	151.15451

the newly added VTOLs. Eqs. (24)–(27) define the decision variables. Note that since the total number of VTOLs or pilots for the entire planning horizon is hard to be decided at the first rolling horizon, we introduce $\mathbf{u}_h$ and $\mathbf{v}_h$ which allow the halfway join of VTOLs and pilots, and abandon the fleet size constraint in the form of Eq. (7). The actual fleet size is finally determined at the end of rolling process.

Note that although $\mathbf{z}$ is optimised in **(P2)**, the decisions for dispatch patterns do not contain $\mathbf{z}$. Thus, the values of $\mathbf{z}$ do not require record in each iteration. Then, the optimisation model (**P2**) can be rolled in following steps to complete the rolling horizon optimisation:

- Step 0: Initialise the cumulative decision variables sets $\mathbf{u}, \mathbf{v}, \mathbf{w}, \mathbf{x}, \mathbf{y} = \mathbf{0}$;
- Step 1: Set the length of ECP and safety margin from to be relatively small values;
- Step 2-0: Iteration of solutions **u**, **v**, **w**, **x**, **y**:
  - Step 2-1: Start with $h = 0$, determine the composition of $\mathcal{B}_h, \mathcal{E}_h$, and run the model in **(P2)** for h to obtain decision variable sets $\mathbf{u}_h, \mathbf{v}_h, \mathbf{w}_h, \mathbf{x}_h, \mathbf{y}_h$. Then, update **u**, **v**, **w**, **x**, **y** by the determined decision variable sets;
  - Step 2-2: If $h = H$, go to Step 3-0. Otherwise, $h = h + 1$;
- Step 3-0: Performance test of solutions **u**, **v**, **w**, **x**, **y**;
  - Step 3-1: Comparing the performance with "entirely predicted demand scenario" where the demand for each TDODP is unknown and "actual demand scenario" where all the passenger demand are known;
  - Step 3-2: If the performance is close to that for "actual demand scenario", stop iteration. Otherwise increase the length of ECP/safety margin and go to Step 2-0.

The collected decision sets **u**, **v**, **w**, **x**, **y** are the final solution in a rolling horizon approach.

4. Case study

4.1. Basic settings

In this section, a network based on GMAS is used to install the modelling approach. Since there has not been any actual vertiport location in GMAS, and the vertiport location placement is not the main concern in this study, we manually select 6 sites as the potential position for air metro vertiports, based on the combined consideration of terrain, per capital income, commuting customer demand and coverage of high-income area. Table 3 shows the sites that are selected as the potential vertiports and the corresponding sets of approx. latitude and longitude. Fig. 4 shows the positions of the vertiports on the map.[2]

In the numerical setting, we adopt the VTOL model of *Joby Aviation*. The reference technical parameters [40,41] are collated and shown in Table 4. For the utilisation cost associated with a human driven VTOL for the planning period, i.e., one day, is the utilisation cost for one VTOL divided by the lifespan (10 years * 365 days), set to be $390.3/day. We refer to [19] regarding the utilisation cost associated

[2] The map and position data are obtained from Google Maps.

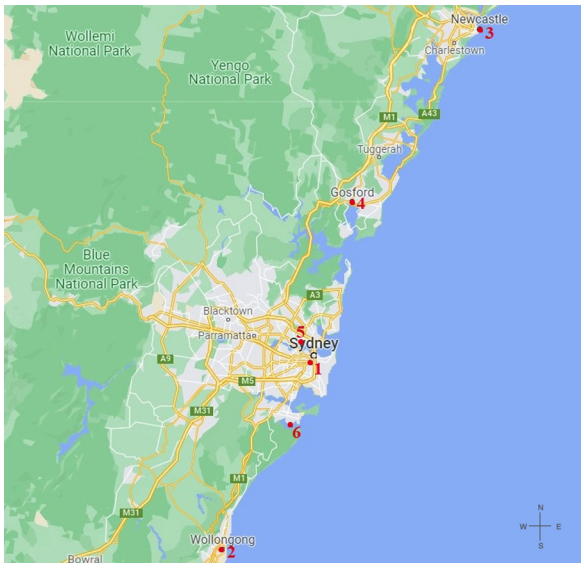

Fig. 4. Position of selected vertiports on map.

Table 4
Parameters of VTOL.

Cruise speed	Range	Capacity	Life span	Price
200 MPH	150 mile	4	10 years	$1.76m

with an autonomous VTOL for the planning period, which is approx. 2.4 times of a human driven one, set to be $936.7/day. The operating cost is set to be $1.4/km, suggested by Reiche et al. [5]. The salary cost associated with employing a pilot for the planning period, i.e., one day, is set to be $158/day [42]. Note that the capacity is 4 passengers, which does not include the pilot. In autonomous air metro scenario, there is no pilot labour cost. However, the fixed utilisation cost associated with providing an autonomous VTOL can be more expensive than a human driven one (in the benchmark case, the utilisation cost for an autonomous VTOLs is 1.2 times of that for a human driven one). Also, extra cost for the service provider may occur in autonomous control equipment (e.g., an autonomous functionality server cost as suggested by Hasan [9]).

A 15-min time step is adopted in this study. Based on the adopted cruise speed, as well as the latitude and longitude of vertiports, the trip time for air metro can be estimated, which is the sum of: (i). cruise time; (ii). trip time for ground phase (i.e., from a passenger's home to origin vertiport/from destination vertiport to the passenger's workplace; (iii). boarding and de-boarding time, take-off and landing time. The cruise time is the Euclidean distance between the origin and destination vertiports divided by cruise speed. The trip time for ground phase is the Manhattan distance (also known as taxicab distance) between home and origin vertiport (or between destination vertiport and workplace) divided by ground traffic speed (set to be 70 km/h). We set the boarding and de-boarding time, take-off and landing time are together 20 minutes. Then, the trip time for each OD pair in a unit of time step can be calculated, as shown in Table 5. Note that the longest trip in the network (between 2# and 3#) is feasible according to the Euclidean distance and the range of VTOLs.

We adopt the assumed demand to simulate the operation network. The demand has two types: the commuting group and the non-commuting group. The commuting groups have a larger demand and a tighter time window, and enter the network only during the morning and evening peak. The non-commuting groups exist throughout the operation hours, with a lower demand and looser time window. The commuting passenger demand for OD pairs is assumed based on the commuting demand for ground transport in GMAS [43]. We adopt the

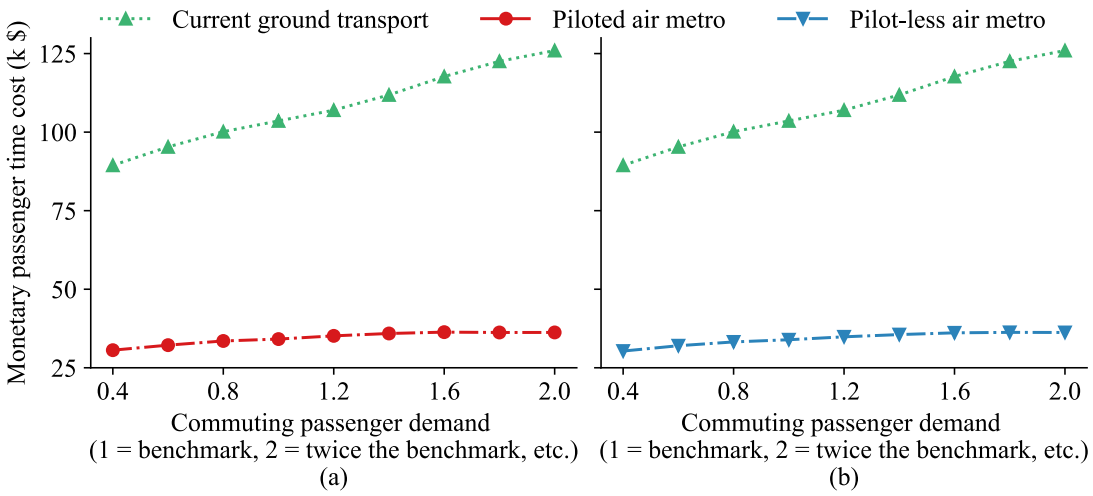

Fig. 5. Monetary passenger time cost of current ground transport and air metro service against demand.

Table 5
Trip time step matrix for air metro OD pairs.

Trip time step	1#	2#	3#	4#	5#	6#
1#	/	2	3	2	2	2
2#	2	/	4	3	2	2
3#	3	4	/	2	3	3
4#	2	3	2	/	2	2
5#	2	2	3	2	/	2
6#	2	2	3	2	2	/

Table 6
Commuting passenger demand matrix during morning peak for OD pairs.

Demand (per time step)	1#	2#	3#	4#	5#	6#
1#	/	1	0	1	0	0
2#	22	/	0	0	3	3
3#	2	0	/	1	2	0
4#	21	0	1	/	7	0
5#	0	0	1	1	/	0
6#	0	2	0	0	0	/

assumptions made by Rajendran and Zack [44], and apply the *k*-means clustering approach to convert the current ground commuting demand into potential air metro demand, based on our assumed vertiport locations. For current ground transport service, the travel time is the sum of ride time and waiting/parking time (set to be 10 min). The ride time is assumed to be the Manhattan distance between the origin and destination divided by ground traffic speed. For each OD pair, we adopt the assumption made by Holden and Goel [6] that "a rider is eligible for a VTOL route if and only if the estimated duration of the route is at least 40% faster relative to the estimated duration of the ground trip". We also assume 1% of total commuters would take air metro service, and the commuting demand evenly enter the network over 2 time steps. Then, the commuting passenger demand per time step for morning peak can be calculated through the adopted data and assumptions, as shown in Table 6. The commuting demand for afternoon peak is considered to be the transpose matrix of Table 6. Moreover, the passenger demands for non-commuting groups have a 50% probability of "no passenger" or "1 passenger" for per time step. The passenger VOT is set to be $39.8/h [45]. For the preferred arrival time window, we consider the temporal lengths of time windows for commuting groups to be one step more than the trip time steps; while those for non-commuting groups are two steps more than the trip time steps. For example, for passengers from 1# to 2#, the trip cost 2 time steps, and thus the time windows for commuting passengers from 1# to 2# are 3 time steps and the time windows for non-commuting passengers from 1# to 2# are 4 time steps. Lastly, the penalty value for unit unsatisfied passenger is set to be 2000.

The operating period for a duty day is set to be [07:00, 23:00]. The pilots are divided into morning and afternoon shifts, where the duty period for morning shift is [07:00, 15:00] and that for afternoon shift is [15:00, 23:00]. Further, in the benchmark setting, we set the maximum fleet size to be 40 VTOLs. The capacity of vertiports, i.e., maximum number of VTOLs landing at the same vertiport at the same time-step, is set to be 10 aircraft.

All ILPs are solved using the commercial solver Gurobi 9.5 interfaced by Julia 1.8.5, whose gap tolerance is 1% (the objective value gap between ILPs and their relaxed linear programming models) to balance computational accuracy and efficiency. The sensitivity analysis on exogenous factors (capacity of vertiports, maximum allowed fleet size, commuting passenger demand, capacity of VTOLs) are then conducted.

Table 7
Computational time of single problems for SNDP models.

Approach	Scenario	Comp. time (s)
Static	Autonomous	1.1
Static	Human driven	2.9
Rolling Horizon	human driven	34.8

4.2. Numerical results

Fig. 5 shows the monetary passenger time cost gap between current ground transport and proposed air metro service, where the cost under the current service is calculated by assuming that value of ground travel time for each OD pair is the Manhattan distance divided by the ground traffic speed (70 km/h). As can be seen from Fig. 5, the monetary passenger time cost can be reduced by 66% (on average) for both scenarios if the air metro service is introduced.

We turn to the utilisation cost of VTOLs. Fig. 6(a) shows results of an experiment which varies the unit utilisation cost of an autonomous VTOL from 0.2 to 2.0 times the benchmark value, with an increment of 0.2. Fig. 6(b) shows results of an experiment which varies the unit utilisation cost of a human driven VTOLs from 1.0 to 2.6 times the benchmark value, with an increment of 0.2. For the experiment on changing utilisation cost of autonomous VTOLs, the system total cost for two scenarios would have a similar value if the utilisation cost of autonomous VTOLs reduces to 0.4 times of the benchmark value; while that for human driven VTOLs shows a critical point of 2.2. The results suggest that under the benchmark values, the autonomous air metro will lead to a higher system total cost. Fig. 7 shows the results of a experiment on changing pilot salary. It can be observed that system total cost remain stable with respect to the changes of salary of pilots.

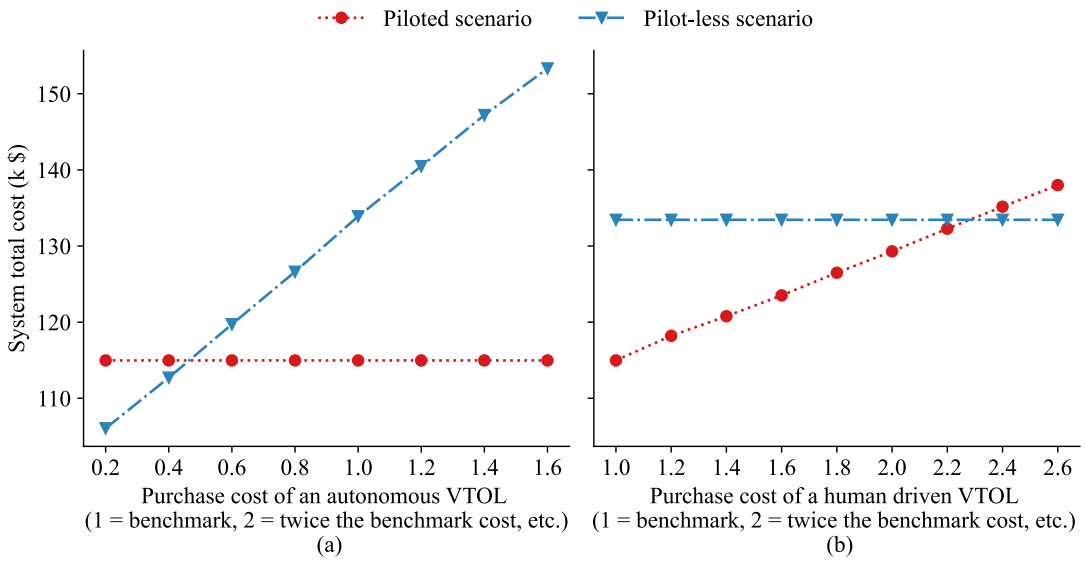

Fig. 6. Comparison of efficiency metrics with the increase of VTOL utilisation cost.

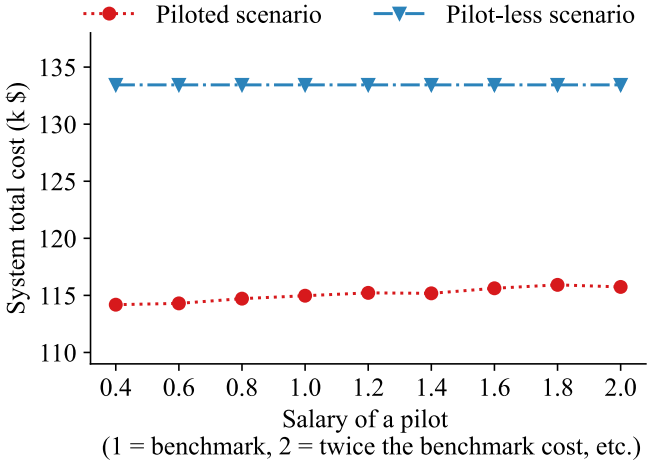

Fig. 7. Comparison of efficiency metrics with the increase of pilot salary cost.

We then conduct a sensitivity analysis to analyse the impact on the performance of the proposed air metro service of three exogenous factors: (i) vertiport capacity, (ii) maximum allowed fleet size, (iii) commuting passenger demand, and analyse their impact on the system total cost in both human driven and autonomous scenarios. We firstly vary the number of vertiports from 4 to 20 with an increment of 2, as shown in Fig. 8. The results suggest that the capacity of vertiport to be no less than 6 VTOLs to reach a trade-off between the performance of service network and the size of vertiports, for both human driven and autonomous scenarios.

We then turn to the experiment on the maximum allowed fleet size by varying the maximum fleet size from 20 to 50, with an increment of 3 VTOLs. As can be seen from Fig. 9, the maximum allowed fleet size is no less than 38 VTOLs when the fleet size is not restricted for both autonomous and human driven scenarios.

For the results for sensitivity analysis on the commuting passenger demand shown in Fig. 10, in the benchmark, the commuting demand is assumed to be 1% of total commuters. In the experiment for commuting passenger demand, we change the demand to be 0.4 to 2 times of the benchmark value (i.e., 0.4% to 2% of total commuting passengers), with an increment of 0.2; while the non-commuting passenger demand remains the same (50% for "1 passenger" and 50% for "no passenger"). The results indicate that in both scenarios, when the commuting demand exceeds 1.2, the penalty becomes critical, and this contributes to a marked increase in total system cost.

4.3. Rolling horizon optimisation for human driven air metro

This section takes the human driven air metro scenario to install the rolling horizon optimisation approach. We consider the passenger demand probability distribution is stochastic and stationary, i.e., the distribution in a time period (e.g., one day) is unit cycle

Larson and Odoni [46] recommended that in urban service systems, the Poisson distribution can be used as a reasonable model for the customer arrival process. Thus, considering that the demand distributions are independent for each group, we assume that they follow the Poisson distribution. Ideally, the rolling horizon should be as long as possible to prevent myopic decisions, but it must also be short enough to permit real-time decisions as well [47]. We set the ECP and safety margin to be 60 min (4 time steps), respectively, as the benchmark. Then, we change the temporal length of ECP and safety margin to determine their impact on solutions. Fig. 11 shows (a) the impact of varied ECP (the safety margin is fixed at 60 min), while Fig. 11(b) studies the different length of safety margin (the ECP is fixed at 60 min). If all the actual demand is known, the system total cost is $116k, which is a lower bound for the rolling horizon approach. Moreover, to compare the cost gap between the rolling horizon optimisation and the static method, we solve the problem **(P0)** with predicted demand, and install the generated solution on the actual demand. The performance of predicted demand scenario is accompanied by a total system cost of approx. $201k (approx. 73% higher than the demand available scenario). As can be seen from both axes, if the length of a single rolling horizon is 90 min (30 for ECP, 60 for safety margin; or 60 for ECP, 30 for safety margin), the performance is unsatisfactory. The total system cost (approx. $210k) is even higher than that for predicted demand scenario. This can be due to the inconsistency between multiple rolling horizons, resulting from the inadequate length of a single rolling horizon. In both axes, when the values of horizontal coordinate increase from 45 to 90, the total system cost shows a considerable decline. However, when the values increase from 90 to 120, there is not any obvious decrease in total system cost. The results suggest it is best to confirm the actual demand at least 45 min prior to departure, and the length of a single rolling horizon should be longer than 150 min. In addition, the increased ECP has a more obvious impact on total system cost than the increase in the safety margin.

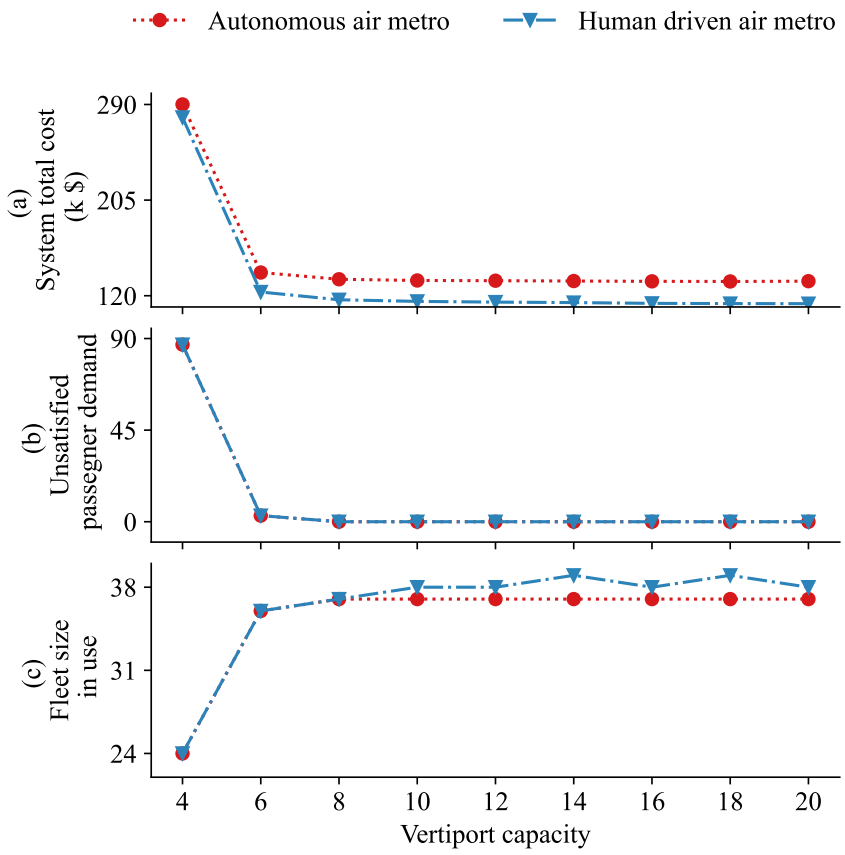

Fig. 8. Sensitivity analysis on vertiport capacity.

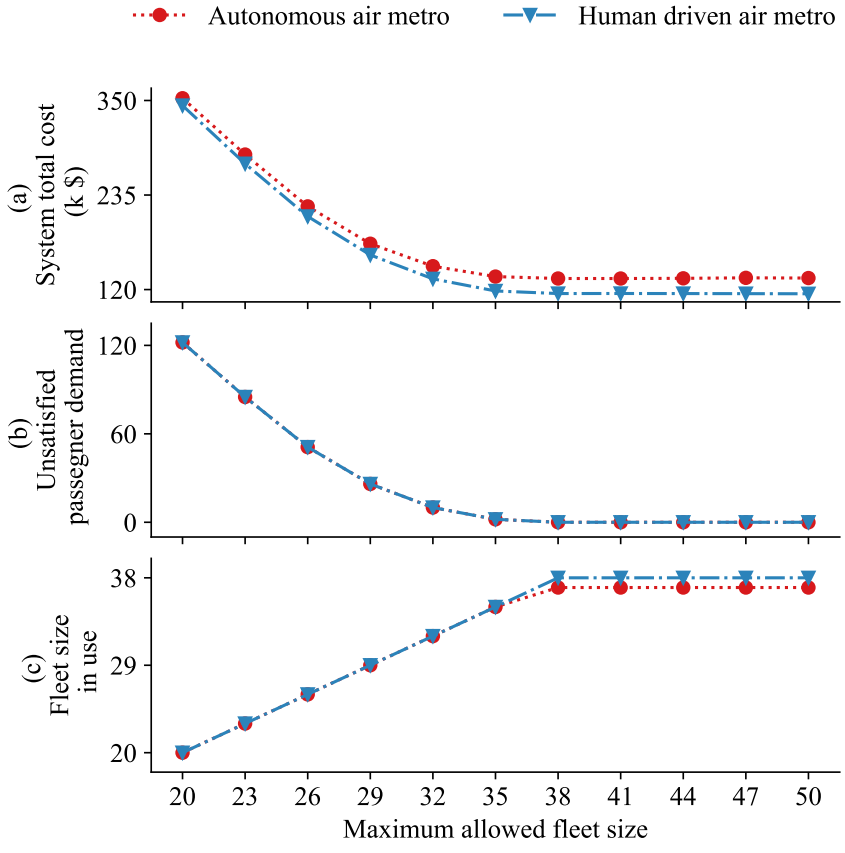

Fig. 9. Sensitivity analysis on maximum allowed fleet size.

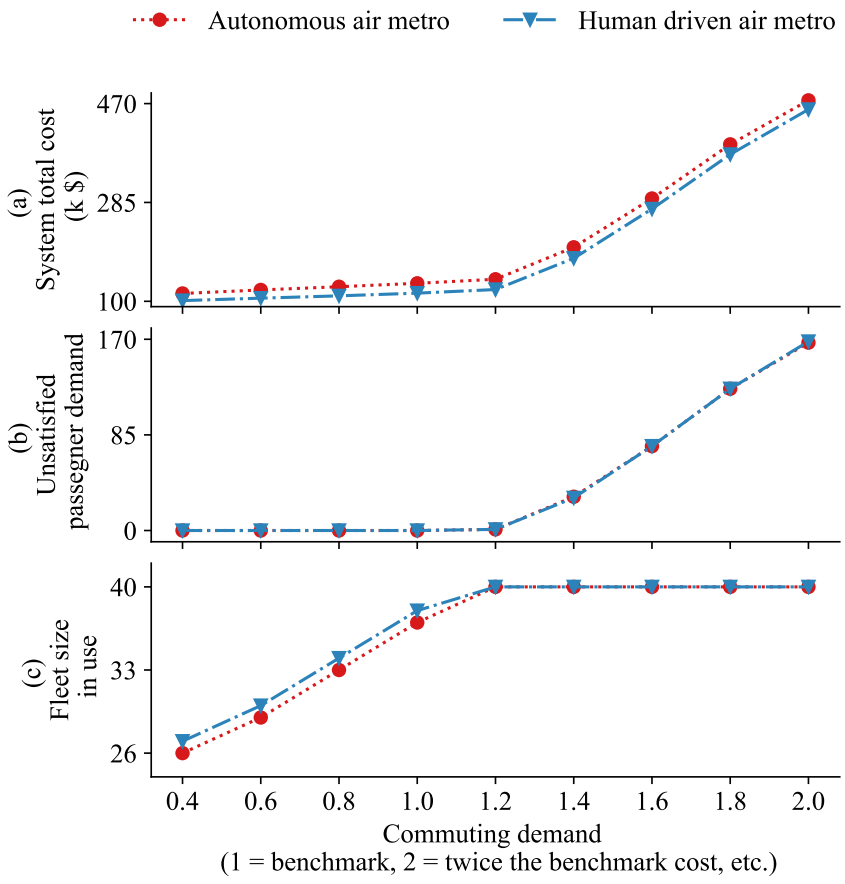

Fig. 10. Sensitivity analysis on commuting passenger demand.

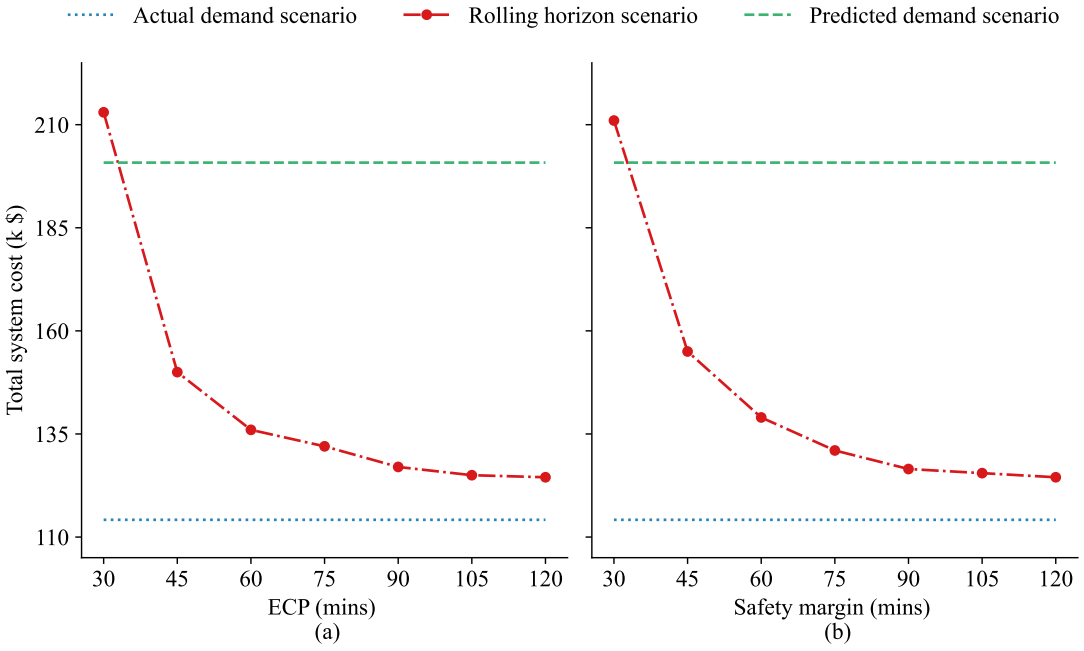

Fig. 11. Performance of rolling horizon optimisation.

The computational efficiency is an important element in the numerical results. Table 7 compares the computational time for ILPs (under benchmark settings) for human driven, autonomous air metro and rolling horizon optimisation (for human driven scenario). The autonomous air metro costs the least computational time because of the absence of pilot scheduling. The rolling horizon cost the most computational time because the problem consists of multiple ILPs. The computational time for rolling horizon study is 12 times that of the static method for a benchmark case.

5. Conclusions

This paper studies a SNDP for the emerging scheduled air metro service. The proposed methods for modelling air metro service in GMAS have shown that the modelling approach can recommend the optimal fleet size, dispatch patterns, and pilot scheduling. For the sensitivity analysis of vertiport capacity, maximum allowed fleet size and commuting passenger demand, the autonomous air metro tends to have a lower system total cost than human driven air metro. The experiments suggest the following key results. In the scenario with an insufficient supply of regular service, the autonomous air metro shows a more obvious increase in the system total cost due to the penalty for unsatisfied passenger demand. It is suggested that the commuting passenger demand is the most significant exogenous factor affecting the system. Comparing the two scenarios reveals that the autonomous air metro service could be the better choice if the utilisation cost of an autonomous aircraft is no greater than 1.2 times that of a human driven one. The experiment that compares the current ground transport and proposed air metro indicates a 66% reduction in the monetary passenger travel time cost with air metro. The results from the rolling horizon optimisation suggest to confirm the actual demand at least 45 min prior to departure. Also, the length of a single rolling horizon should be no shorter than 150 min. As for the computational time, the rolling horizon case study costs 12 times more than the static method to solve a benchmark problem.

The model aimed to minimise the operating costs for the service provider as well as the monetary passenger travel costs. Another aim of this study was to analyse and compare the costs of human driven and autonomous air metro scenarios, where human driven air metro has a labour cost for pilots, and autonomous air metro may have a higher vehicle manufacturing cost and automation cost. Given that air metro is geared towards business users with high VOT, it is important to understand the feasible lead time between booking and departure in order to understand the optimal balance between operations and passenger benefits. Moreover, it is feasible to ask passengers to confirm their reservations via a mobile app several hours prior to departure time, which would allow the operator to determine the actual demand for the trip. Thus, this paper utilised the method of rolling horizon optimisation.

There are several directions in which this study can be extended. First, this study considered six vertiports, which were suitable for the case study context. The case of dense vertiports (e.g. 100-300 vertiports located in high-traffic areas of much larger city such as New York as suggested by Hasan [9]) could considerably increase the computation complexity. The proposed approach may be less applicable for very large-scale problems. Future research may require a more efficient meta-heuristic. Second, this study has not investigated the service offered from multiple providers with different price and service quality. A future research may propose a platform from the vertiports' perspective incorporating multiple air metro companies. Third, this paper does not model a remotely-human driven operations scenario, which can be an intermediate step between pilot and autonomous operations. Therefore, future research can apply the current framework to consider this alternative, which may involve cost savings by spreading the pilot load over multiple vehicles. From the perspective of SNDP design, in the case of the "in-person safety pilot", one can draw similar conclusions as the human driven scenario presented in this study. Fourth, as this study's focus was on the SNDP design, market variables were not internalised in the modelling framework. However, clearly, the pricing from the air metro service can affect the passenger demand. The pricing will be determined by demand and supply conditions of the market, and these considerations are natural extensions of this study, especially if the focus is on market analysis incorporating substitute travel modes. Fifth, this study assumes the VTOL technology in consideration for the near future is limited to relatively short-distance travel with small vehicles (up to 5 people) rather than longer flights, which are better serviced by conventional aircraft with large capacity. Last, this air metro service is geared towards business users, and the performance of solutions under worst-case of the uncertain conditions requires further robust optimisation research. Future studies may develop solution approaches for robust air metro service network design problem with integer flow variables.

Declaration of competing interest

The authors declare that they have no known competing financial interests or personal relationships that could have appeared to influence the work reported in this paper.

Data availability

No data was used for the research described in the article.

Acknowledgements

Dr. Tay Koo would like to thank Malcolm Good and Rodney Hyde from the UNSW Flying Operations Unit for helpful advice during the conceptualisation phase of this research.

Dr. Wei Liu would like to acknowledge the support from The Hong Kong Polytechnic University (P0039246, P0040900, P0041316).

References

[1] Danielle Gagne, NASA has changed urban air mobility to advanced air mobility, should the industry follow suit? 2020, URL https://www.commercialuavnews.com/infrastructure/nasa-has-changed-urban-air-mobility-to-advanced-air-mobility-should-the-industry-follow-suit.

[2] Jordi Pons-Prats, Tanja Živojinović, Jovana Kuljanin, On the understanding of the current status of urban air mobility development and its future prospects: Commuting in a flying vehicle as a new paradigm, Transp. Res. E 166 (2022) 102868.

[3] David Learmount, Waiting for the eVTOL-taxi rank, 2021, URL https://www.aerosociety.com/news/waiting-for-the-evtol-taxi-rank/.

[4] Rohit Goyal, Colleen Reiche, Chris Fernando, Adam P. Cohen, Advanced air mobility: Demand analysis and market potential of the airport shuttle and air taxi markets, Sustainability 13 (13) (2021) 7421.

[5] Colleen Reiche, Rohit Goyal, Adam P. Cohen, Jacquie Serrao, Shawn Kimmel, Chris Fernando, Susan A. Shaheen, Urban air mobility market study, Technical report, Booz-Allen and Hamilton, Inc., 2018.

[6] Jeff Holden, Nikhil Goel, Fast-forwarding to a future of on-demand urban air transportation, Technical report, Uber Elevate, 2016.

[7] Gregor Grandl, Martin Ostgathe, Jan Cachay, Stefan Doppler, John Salib, Han Ross, The future of vertical mobility, Technical report, Porsche Consulting, 2018.

[8] Pavan Yedavalli, Jessie Mooberry, An assessment of public perception of urban air mobility, Technical report, Airbus UTM, 2019.

[9] Shahab Hasan, Urban air mobility market study, Technical report, Crown Consulting, Inc., 2018.

[10] Steve Bradford, Concept of operations for urban air mobility, Technical report, Federal Aviation Administration NextGen Office, 2020.

[11] Adam P. Cohen, Susan A. Shaheen, Emily M. Farrar, Urban air mobility: History, ecosystem, market potential, and challenges, IEEE Trans. Intell. Transp. Syst. 22 (9) (2021) 6074–6087.

[12] Ahmad Baubaid, Natashia Boland, Martin Savelsbergh, The value of limited flexibility in service network designs, Transp. Sci. 55 (1) (2021) 52–74.

[13] Miloš Balać, Amedeo R. Vetrella, Kay W. Axhausen, Towards the integration of aerial transportation in urban settings, in: Arbeitsberichte Verkehrs-Und Raumplanung, Vol. 1266, IVT ETH Zurich, 2017.

[14] Taha Hossein Rashidi, Travis Waller, Kay Axhausen, Reduced value of time for autonomous vehicle users: Myth or reality? Transp. Policy 95 (2020) 30–36.

[15] Caroline Pigeon, Aline Alauzet, Laurence Paire-Ficout, Factors of acceptability, acceptance and usage for non-rail autonomous public transport vehicles: A systematic literature review, Transp. Res. F 81 (2021) 251–270.
[16] Krishna Murthy Gurumurthy, Kara M. Kockelman, Modeling Americans' autonomous vehicle preferences: A focus on dynamic ride-sharing, privacy & long-distance mode choices, Technol. Forecast. Soc. Change 150 (2020) 119792.
[17] Laurie A. Garrow, Brian J. German, Caroline E. Leonard, Urban air mobility: A comprehensive review and comparative analysis with autonomous and electric ground transportation for informing future research, Transp. Res. C 132 (2021) 103377.
[18] Ugur Eker, Grigorios Fountas, Panagiotis Ch Anastasopoulos, An exploratory empirical analysis of willingness to pay for and use flying cars, Aerosp. Sci. Technol. 104 (2020) 105993.
[19] Satadru Roy, Apoorv Maheshwari, William A. Crossley, Daniel A. DeLaurentis, Future regional air mobility analysis using conventional, electric, and autonomous vehicles, J. Air Transp. 29 (3) (2021) 113–126.
[20] Christelle Al Haddad, Emmanouil Chaniotakis, Anna Straubinger, Kay Plötner, Constantinos Antoniou, Factors affecting the adoption and use of urban air mobility, Transp. Res. A 132 (2020) 696–712.
[21] Karolin Schweiger, Lukas Preis, Urban air mobility: Systematic review of scientific publications and regulations for vertiport design and operations, Drones 6 (7) (2022) 179.
[22] Quan Shao, Mengxue Shao, Yang Lu, Terminal area control rules and eVTOL adaptive scheduling model for multi-vertiport system in urban air mobility, Transp. Res. C 132 (2021) 103385.
[23] Kai Wang, Alexandre Jacquillat, Vikrant Vaze, Vertiport planning for urban aerial mobility: An adaptive discretization approach, Manuf. Serv. Oper. Manag. 24 (6) (2022) 3215–3235.
[24] Wenjuan Hou, Tao Fang, Zhi Pei, Qiaochu He, Integrated design of unmanned aerial mobility network: A data-driven risk-averse approach, Int. J. Prod. Econ. 236 (2021) 108131.
[25] Landon C. Willey, John L. Salmon, A method for urban air mobility network design using hub location and subgraph isomorphism, Transp. Res. C 125 (2021) 102997.
[26] Akhouri Amitanand Sinha, Suchithra Rajendran, A novel two-phase location analytics model for determining operating station locations of emerging air taxi services, Decis. Anal. J. 2 (2022) 100013.
[27] Hyelim Shin, Taesik Lee, Hyun Rok Lee, Skyport location problem for urban air mobility system, Comput. Oper. Res. 138 (2022) 105611.
[28] Liting Chen, Sebastian Wandelt, Weibin Dai, Xiaoqian Sun, Scalable vertiport hub location selection for air taxi operations in a metropolitan region, INFORMS J. Comput. 34 (2) (2022) 834–856.
[29] Suchithra Rajendran, Sharan Srinivas, Air taxi service for urban mobility: a critical review of recent developments, future challenges, and opportunities, Transp. Res. E 143 (2020) 102090.
[30] Satadru Roy, Mark T. Kotwicz Herniczek, Caroline E. Leonard, Ayush Jha, Nathan Wang, Brian J. German, Laurie A. Garrow, A multi-commodity network flow approach for optimal flight schedules for an airport shuttle air taxi service, in: AIAA Scitech 2020 Forum, Orlando, U.S., 2020, p. 0975.
[31] Suchithra Rajendran, Real-time dispatching of air taxis in metropolitan cities using a hybrid simulation goal programming algorithm, Expert Syst. Appl. 178 (2021) 115056.
[32] Mehdi Bennaceur, Rémi Delmas, Youssef Hamadi, Passenger-centric urban air mobility: Fairness trade-offs and operational efficiency, Transp. Res. C 136 (2022) 103519.
[33] Rohit Goyal, Adam P. Cohen, Advanced air mobility: Opportunities and challenges deploying eVTOLs for air ambulance service, Appl. Sci. 12 (3) (2022) 1183.
[34] Satadru Roy, Mark T. Kotwicz Herniczek, Caroline E. Leonard, Brian J. German, Laurie A. Garrow, Flight scheduling and fleet sizing for an airport shuttle air taxi service, J. Air Transp. 30 (2) (2022) 49–58.
[35] Konstantinos Gkiotsalitis, Stop-skipping in rolling horizons, Transportmetrica A: Transp. Sci. 17 (4) (2021) 492–520.
[36] Imke C. Kleinbekman, Mihaela Mitici, Peng Wei, Rolling-horizon electric vertical takeoff and landing arrival scheduling for on-demand urban air mobility, J. Aerosp. Inf. Syst. 17 (3) (2020) 150–159.
[37] Hong K. Lo, Kun An, Wei Hua Lin, Ferry service network design under demand uncertainty, Transp. Res. E 59 (2013) 48–70.
[38] Daniel Espinoza, Renan Garcia, Marcos Goycoolea, George L Nemhauser, Martin WP Savelsbergh, Per-seat, on-demand air transportation part I: Problem description and an integer multicommodity flow model, Transp. Sci. 42 (3) (2008) 263–278.
[39] Teodor Gabriel Crainic, Mike Hewitt, Michel Toulouse, Duc Minh Vu, Service network design with resource constraints, Transp. Sci. 50 (4) (2016) 1380–1393.
[40] jobyoffi Joby Aviation (n.d.). URL: https://www.jobyaviation.com/.
[41] Jeremy Bogaisky, Electric air taxi maker joby goes public, offering investors sky-high potential-and risk, 2021, URL https://www.forbes.com/sites/jeremybogaisky/2021/08/11/joby-stock-spac-nyse/?sh=27240c487a41/.
[42] indeedsalary Indeed (n.d.), 'Pilot salary in australia'. URL: https://au.indeed.com/career/pilot/salaries/.
[43] tfNSW, Journey to work, 2011, URL https://opendata.transport.nsw.gov.au/dataset/journey-work-jtw-2011/.
[44] Suchithra Rajendran, Joshua Zack, Insights on strategic air taxi network infrastructure locations using an iterative constrained clustering approach, Transp. Res. E 128 (2019) 470–505.
[45] tfNSW, Transport for NSW economic parameter values, 2020, URL https://www.transport.nsw.gov.au/news-and-events/reports-and-publications/tfnsw-economic-parameter-values/.
[46] Richard C. Larson, Amedeo R. Odoni, Urban Operations Research, Transportation research board, 1981.
[47] Wuhua Hu, Jianfeng Mao, Keji Wei, Energy-efficient rail guided vehicle routing for two-sided loading/unloading automated freight handling system, European J. Oper. Res. 258 (3) (2017) 943–957.